Seismic Interferometry Applied to Seismic Background-Noise Field Data

Deyan Draganov[(1)], Kees Wapenaar[(1)], Wim Mulder[(1,2)], Johannes Singer[(2)], and Arie Verdel[(2)]
[(1)]Department of Geotechnology, Delft University of Technology, Delft, The Netherlands,
[(2)]Shell International E&P, Rijswijk, The Netherlands

June 14, 2006

KEY WORDS: Seismic Interferometry, field data, crosscorrelation, seismic background noise, reflection response

ABSTRACT

One of the applications of Seismic Interferometry (SI) is the reconstruction of the Earth's reflection response from the crosscorrelation of seismic background noise recorded at the surface. In recent years, several authors have derived the relations that govern this process. The quality of the reconstruction has been extensively examined with numerical modeling results. Several authors have applied the method to real data for the reconstruction of surface waves.

We applied SI to background-noise field data recorded in a desert area. The reconstructed results show several coherent events – inclined and nearly horizontal. The inclined coherent events are interpreted as reconstructed surface waves. The nearly horizontal coherent events appear to align well with reflections from an active survey along the same line. Therefore, we interpret these events as reconstructed reflections.

INTRODUCTION

If one looks at a raw seismic reflection (exploration) record, one notices that apart from the desired reflections and (mostly undesired) surface waves, there are a lot of other events that are normally described as "seismic background noise". And as a result, one of the goals of a data processor is to eliminate this unwanted noise. But there is also useful information in the seismic noise – it may contain propagating waves (transmission response) even though these are not a result of conventional exploration sources. Claerbout (1968) was the first to show how to make use of the seismic noise. He proved that for a 1D acoustic medium the autocorrelation of the transmission response can reconstruct the reflection response of the medium. Later, he stated the conjecture that in the case of a 3D acoustic medium, one should crosscorrelate the observed at the surface transmission response to reconstruct the reflection response. Wapenaar et al. (2002) proved Claerbout's conjecture for any 3D inhomogeneous acoustic medium (later also for elastic), starting with one-way wavefield reciprocity theorems. They showed how to reconstruct the reflection response in the case of deterministic as well as white-noise sources in the subsurface. At about the same time, other authors derived similar relations using different techniques for applications in different fields (Weaver and Lobkis, 2001; Schuster, 2001; Derode et al., 2003; Snieder, 2004) and as a result different terminology was introduced for the same process. To avoid confusion, it was proposed, in a special issue of Geophysics dedicated to these techniques, to use the term Seismic Interferometry (SI) for reconstruction through crosscorrelation (Geophysics, July-August issue of 2006).

One of the applications of SI for exploration is the reconstruction of the reflection response from the crosscorrelation of seismic background noise recorded at the surface. In the normal seismic processing scheme, such noise is discarded. Several authors have shown the successful application of SI for the reconstruction of surface waves from seismic noise (Campillo and Paul, 2003; Sabra et al., 2005; Shapiro et al., 2005).

In the following sections, we present results from the application of SI to seismic background-noise data recorded in a desert area. The aim of the experiment was to reconstruct reflection records that can be used in exploration, for example in frontier exploration areas.

FIELD EXPERIMENT DESCRIPTION

In 2005, Shell carried out a small field experiment to test the applicability of SI with seismic background noise for reconstruction of the reflection response. The experimental set-up consisted of 17 standard industry 3-component geophones arranged in a single line. The geophone spacing was 50 m and the time-sampling rate was 4 ms. The array was planted in a desert area. The

particular site was chosen so that there would be an active seismic survey available along the line to allow for verification of the reconstructed results and that the cultural noise was minimal during the recording of the background noise. Standard exploration equipment was used, which allowed for a maximum record length of 70 s. The background noise recording was then interrupted for 30 s to store the already acquired record. To be able to reconstruct the reflection response of a medium from crosscorrelation of noise, one needs time series at least of the order of hours. For this reason, 524 70-seconds records were acquired amounting to about 10 hours of seismic background-noise data.

RECONSTRUCTION OF THE REFLECTION RESPONSE

To reconstruct the reflection response from the recorded background-noise data, we used the SI relation as derived in Wapenaar and Fokkema (2006) using two-way wavefield reciprocity. In the frequency domain this relation reads

$$2\Re\left\{\hat{G}^{\nu,t}_{p,q}\left(\mathbf{x}_A,\mathbf{x}_B,\omega\right)\right\}\hat{S}\left(\omega\right)\propto \left\langle\left\{\hat{\nu}^{obs}_{p}\left(\mathbf{x}_A,\omega\right)\right\}^{*}\hat{\nu}^{obs}_{q}\left(\mathbf{x}_B,\omega\right)\right\rangle, \quad (1)$$

where $\hat{G}^{\nu,t}_{p,q}\left(\mathbf{x}_A,\mathbf{x}_B,\omega\right)$ is the Green's function observed at the surface at $\mathbf{x}_A$ due to a source at the surface at $\mathbf{x}_B$ with a source spectrum $\hat{S}\left(\omega\right)$ equal to the power spectrum of the background noise. This Green's function represents the observed p-component of the particle velocity (ν) due to a traction source (t) acting in the q-direction ($p,q=1,2,3$). As both the source and receiver are at the surface, the Green's function is the surface shot response including the reflections of the medium. At the right-hand side of relation 1, $\langle\cdot\rangle$ stands for spatial ensemble average and $\hat{\nu}^{obs}_{p}\left(\mathbf{x}_A,\omega\right)$ denotes the observed p-component of the particle velocity that one will measure at the surface at $\mathbf{x}_A$ when all subsurface noise sources are acting simultaneously. As the receiver is at the surface and the sources in the subsurface, $\hat{\nu}^{obs}_{p}\left(\mathbf{x}_A,\omega\right)$ represents the transmission response of the medium. Relation 1 states that by crosscorrelating (in the time domain) the observed transmission responses at two points from subsurface seismic background-noise sources, one can obtain the reflection response and its anti-causal version at one of the points as if a source were present at the other point. In the derivation of this relation, it was assumed that the medium along the subsurface sources is homogeneous, hence ρ and c_P are constant. If the noise sources are present in the subsurface so that they illuminate the observation points from all directions, then the causal (at positive times) and the anti-causal (at negative times) part of the reflection reponse will be the same and to obtain the reflection response we can just mute the negative times.

According to relation 1, to reconstruct the vertical component of the particle velocity from a vertical traction source, we have to correlate the vertical components of the recorded background-noise data. We used the following procedure. One 70-seconds recording (a background-noise panel) was energy-normalized. Then, we extracted one of its traces (a master trace, in Figure 1 at $x_1 = 0$ m) and crosscorrelated it with the same background-noise panel to obtain a so-called correlation panel. We repeated this for all 524 background-noise panels by always taking the master trace at the same location. The resulting 524 correlation panels were then summed to obtain a final reconstructed reflection shot gather. Due to the energy-normalization of the background-noise panels, in the summation process all the correlation panels contributed to the final result. Inspection of the frequency spectrum of the background-noise panels showed that the useful information is mainly below 12 Hz. For this reason, the reconstructed results were band-pass filtered between 2 and 10 Hz. Figures 1(a)-(e) show the intermediate results from building the final reconstructed common-shot gather as if from a source at horizontal position $x_1 = 0$ m. The panels were clipped to bring forward the events at later times. One can appreciate how the addition of extra background-noise panels, which effectively means having longer recording times, includes more subsurface information and increases the signal-to-noise ratio. Due to the short array spread and the low frequencies and due to the fact that the geology in the area is composed of nearly horizontal layers, the reflection events below 1.5 s should appear nearly horizontal.

Figures 1(a)-(e) show the first 10 s of the causal part of the reconstructed results, while the negative times were muted. This is justified if the subsurface background noise sources illuminate the recording array from all directions. In reality, we could not know if this is really so. That is why we also looked at the negative times. Figure 2(a) shows the first 10 s of the reversed-in-time anti-causal part of the reconstructed result for a simulated source at $x_1 = 0$ m, Figure 2(b) shows the first 10 s of the causal part for the same reconstruction, and Figure 2(c) shows the sum of (a) and (b). One can clearly see that the causal and the anti-causal part are not the same. That is why one should look at their sum, which should give a more complete reconstruction.

By changing the position of the master trace along the receiver array and taking the vertical components of the background-noise recordings, we reconstructed common-shot gathers with simulated sources positions at $x_1 = 0, 100, 150, ..., 800$ m. (Note that the second geophone was dead.) Figures 3(a) and (b) show the first 10 s of the reconstructed common-shot gathers for simulated shots at $x_1 = 150$ and $x_1 = 350$ m, respectively, after summing the causal and anti-causal parts of the respective reconstructed results. In principle, having reconstructed all sixteen shot gathers could allow us to perform velocity analysis. In practice this

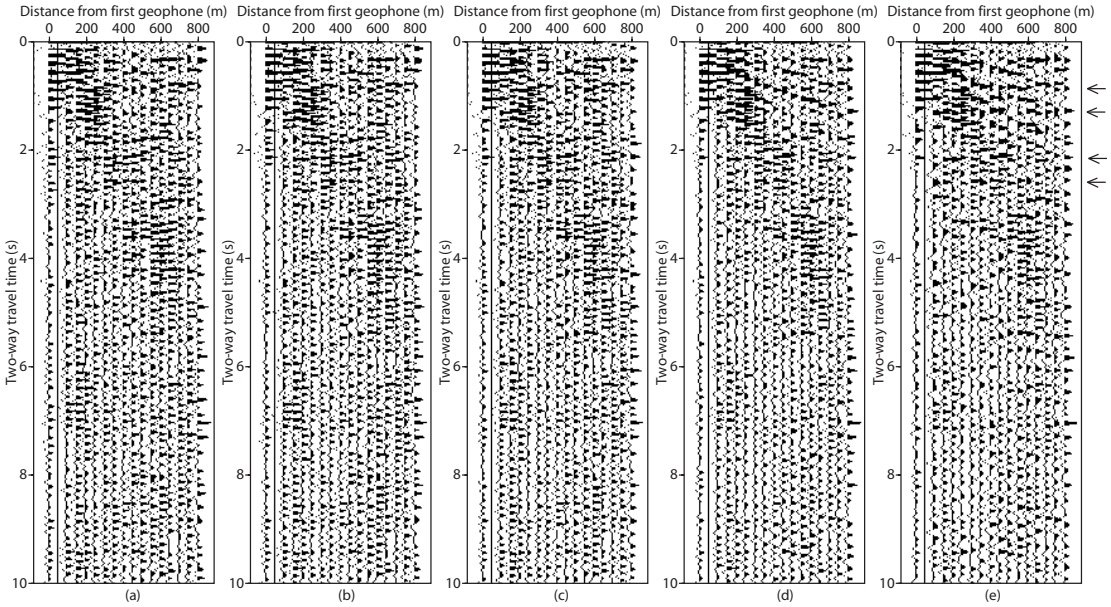

Figure 1: Gradual building of the reconstructed vertical particle velocity as if from a vertical traction source at $x_1 = 0$ m. The individual panels show the first 10 s of the causal part of the reconstruction of the common-shot gather after summation of (a) 100, (b) 200, (c) 300, (d) 400 and (e) 500 correlation panels. The arrows point to events that can be interpreted as nearly horizontal reflection arrivals. These arrivals will become clearer in the following figures.

was difficult due to the negligible moveout. Therefore we took two other approaches based on the assumption that the subsurface is composed of horizontal layers.

For the first approach, we sorted the reconstructed common-shot gathers into common-offset gathers. The traces in the individual offset gathers were summed together, the resulting trace was divided by the number of summed traces and assigned to the corresponding offset. This operation should bring forward any coherent events that were present in the reconstructed results. The results of the common-offset stack operation are shown in Figures 4(a)-(c). Automatic Gain Control (AGC) was applied to bring forward the late arrivals and offsets larger than 650 m were not used. Figures 4(a) and 4(b) show the first 10 s of the reversed-in-time anti-causal part and the first 10 s of the causal part of the common-offset stack panel, respectively. The negative value of the offset denotes geophones to the left of the simulated shot position. Indeed, now one sees more clearly the inclined and horizontal coherent events that were also visible, to different degrees, on the individual shot gather panels. We interpreted the inclined events as surface waves. The horizontal events could be interpreted as reflections (primaries or multiples). However, surface waves with a propagation front parallel to the receiver array could also produce horizontal coherent events. We come back to this later. What is also interesting to observe in Figure 4, is the mirror symmetry of (a) and (b). This could be a hint that the background-noise sources were mainly concentrated on one side of the receiver array. When the subsurface consists of horizontal layers, the negative and positive offsets should exhibit the same coherent events. One can see that the sum of (a) and (b) will produce this result, which shows that indeed the summation of the causal and anti-causal part of the reconstructed records will give the complete picture. By summing (a) and (b) and further summing the positive and negative offsets, the signal-to-noise ratio is further increased (see Figure 4(c)). For comparison, 4(d) shows the common-offset stack result from finite-difference elastic forward modeling, for which we used a simplified 1D model based on the results from the active survey. This panel is included to show the shape of the expected coherent arrivals (and in this way to help the interpretation of Figure 4(c)) and should not be used for travel-time comparison.

The second approach is a brute stack of the traces in each individual reconstructed common-shot gather. The resulting trace is assigned at the position of the simulated shot position of the corresponding shot gather. This operation is equivalent to a physical plane-wave experiment, where the receiver array would emit a plane wave and record its response. The result of this approach is that (nearly) horizontal coherent events will be amplified. At the same time, random noise, inclined coherent events and reflections with moveout will be suppressed. The results of this operation are shown in Figure 5(b). Note that AGC was used to boost the later arrivals. One can see clear presence of several coherent horizontal events, which can be reconstructed reflections. These events are pointed out with arrows. The first two of the horizontal events were not that clearly visible on the common-offset stack panel (Figure 5(a)).

We compared the results from the common-offset stack and the brute stack with a Post-Stack Time Mi-

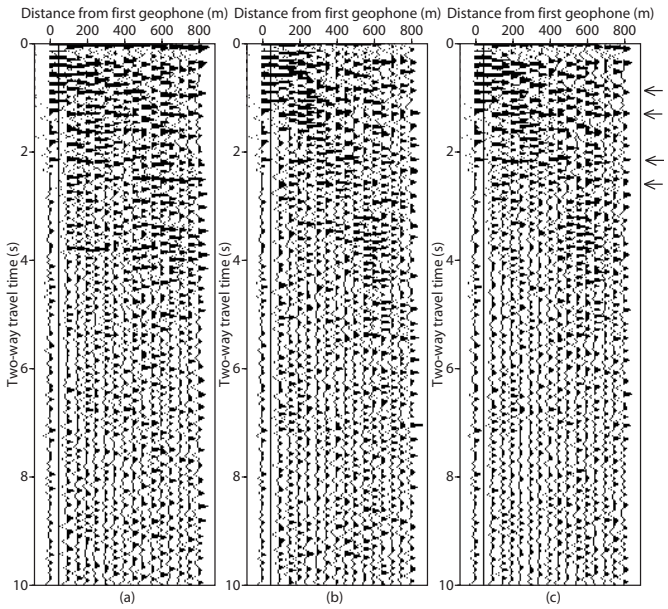

Figure 2: Reconstructed vertical particle velocity reflection response as if from a vertical traction source at $x_1 = 0$ m. (a) Reconstructed coherent events in the anti-causal part of the final correlation panel (negative times). (b) Reconstructed coherent events in the causal part (positive times). (c) Result of the summation of (a) and (b).

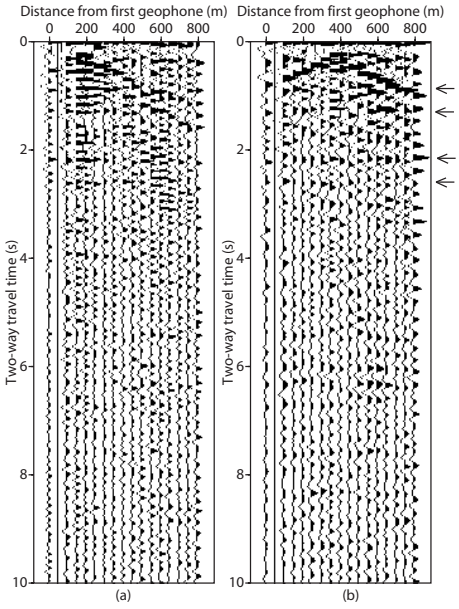

Figure 3: (a) Reconstructed vertical particle velocity reflection response as if from a vertical traction source at $x_1 = 150$ m after summing the causal and the anti-causal parts. (b) Same as (a) but for a source at $x_1 = 350$ m.).

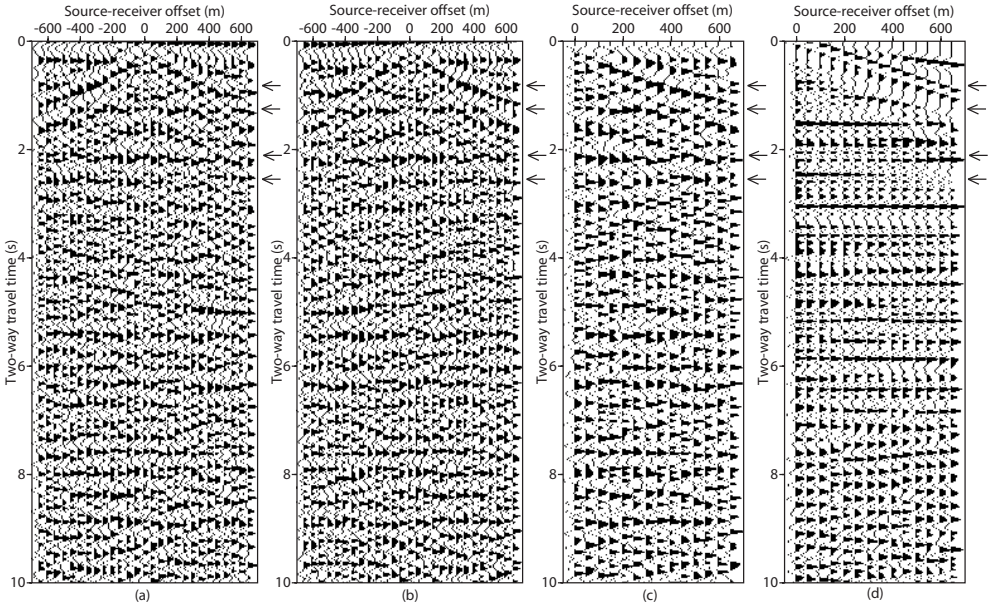

Figure 4: First 10 s of a common-offset stack panel obtained by resorting the reconstructed shot gathers into common-offset gathers and stacking of the traces in the common-offset gathers. AGC was applied to bring forward the later arrivals. (a) Reversed-in-time anti-causal part of the reconstructed common-offset stack panel. (b) Causal part of the reconstructed common-offset stack panel. (c) The result after adding (a) and (b) and further summing the positive and negative offsets. (d) Common-offset stack panel produced from finite-difference modeling using a 1D elastic subsurface model derived from the active survey. After 4 seconds, artefacts appear that are caused by the absorbing boundary conditions. This modeling result is included to show the shape of the expected coherent arrivals and should not be used for travel-time comparison.

grated (PSTM) section (Figure 5(c)) from an active reflection survey along the same line of geophones. The active survey PSTM data was low-pass filtered till 20 Hz as it did not contain information below 8 Hz. Despite the difference in frequency content, the comparison of Figures 5(a)-(b) with 5(c) shows that the four coherent horizontal events pointed out with the arrows can potentially be reconstructed reflections. The active reflection data was 6 s long and therefore that did not allow a comparison of later arrivals.

As noted earlier, the reconstructed horizontal coherent events could in principle also be caused by surface waves propagating with a wavefront parallel to the receiver array. The following arguments show that this is not very likely. One should look at the 3-component background-noise records (in the band between 2 and 10 Hz) and look for (nearly) horizontal arrivals, which after crosscorrelation would produce the horizontal coherent events in the reconstructed shot gathers. In the background-noise recordings, surface waves should be registered on at least two of the three components of the geophones. We looked at the background-noise recordings for (nearly) horizontal arrivals. We found such arrivals in several of the background-noise panels. Most of these arrivals had the same amplitude as the rest of the events in the panels, but there were a few with amplitude 5 to 50 times higher (note that after normalization this difference in amplitude will not matter). Figure 6 shows horizontal arrivals found in panel 66 and starting at around 12 s. One can see that the first arrival in this figure is only registered on the vertical component, which points out that this is most likely a plane body wave arrival.

CONCLUSIONS

We applied Seismic Interferometry to ten hours of passively acquired seismic background-noise data consisting of 524 noise panels each of which was 70 seconds long. The crosscorrelation produced coherent events in the reconstructed shot gathers. The more noise panels were included in the reconstruction process, the better the reconstructed result. Coherent horizontal and inclined arrivals appeared in the causal as well as in the anti-causal part of the reconstructed shot gathers. The causal and anti-causal parts were not symmetric, which means that the background-noise sources do not illuminate the receiver array uniformly from all directions. The crosscorrelation results were band-pass filtered between 2 and 10 Hz. Because of these low frequencies and because of the short length of the receiver array, reflection events below 1.5 s should appear nearly horizontal. We interpreted the reconstructed inclined coherent events as surface waves. As the geology in the area is nearly horizontally layered, we applied two stacking methods that amplify the reconstructed coherent events - common-offset stack and brute stack. Both results were compared with a Post-stack time migrated section from an active reflection survey. The reconstructed horizontal coherent events appear to align very well with imaged reflectors from the active survey. Based on this and on the analysis of the 3-component background-noise data, we interpreted the reconstructed horizontal events as reconstructed reflections.

ACKNOWLEDGMENTS

This research is supported by The Netherlands Research Centre for Integrated Solid Earth Sciences ISES, by the Technology Foundation STW, applied science division of NWO, and the technology program of the Ministry of Economic Affairs (grant DTN4915). The authors would like to thank Ranajit Ghose, Fons Ten Kroode, and Gerard Herman for the helpful discussions.

REFERENCES

Campillo, M., and Paul, A., 2003, Long-range correlations in the diffuse seismic coda, *Science*, **299**, 547–549.

Claerbout, J. F., 1968, Synthesis of a layered medium from its acoustic transmission response, *Geophysics*, **33**, 264–269.

Derode, A., Larose, E., Tanter, M., de Rosny, J., Tourin, A., Campillo, M., and Fink, M., 2003, Recovering the Green's function from field-field correlations in an open scattering medium, *Journal of the Acoustic Society of America*, **113**, 2973–2976.

Sabra, K. G., Gerstoft, P., Roux, P., Kuperman, W. A., and Fehler, M. C., 2005, Extracting time-domain Green's function estimates from ambient seismic noise, *Geophysical Research Letters*, **32**, 10.1029/2004GL021862.

Schuster, G. T., 2001, Theory of daylight/interferometric imaging: tutorial, 63th Conference and Exhibition, EAGE, Extended abstracts, A–32.

Shapiro, N. M., Campillo, M., Stehly, L., and Ritzwoller, M. H., 2005, High-resolution surface wave tomography from ambient seismic noise; *Science*, **307**, 1615–1618.

Snieder, R., 2004, Extracting the Green's function from the correlation of coda waves: a derivation based on stationary phase, *Physical Review E*, **69**, 046610–1–046610–8.

Wapenaar, C. P. A., Thorbecke, J. W., Draganov, D., and Fokkema, J. T., 2002, Theory of acoustic daylight imaging revisited, 72nd Annual International Meeting, SEG, Expanded abstracts, ST 1.5.

Wapenaar, C. P. A., and Fokkema, J., 2006, Green's functions representations for seismic interferometry, *Geophysics*, **in press**.

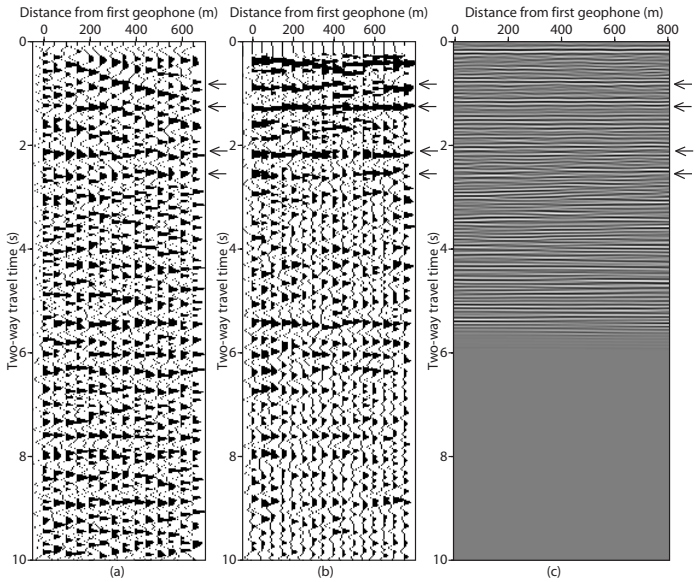

Figure 5: (a) First 10 s of the reconstructed common-offset stack panel (same as in Figure 4(c). (b) First 10 s of a brute stack of the individual reconstructed shot gathers. AGC was used to boost the later arrivals. (c) Post-Stack Time-Migration image result from an active reflection survey in the same area (low-pass filtered up to 20 Hz).

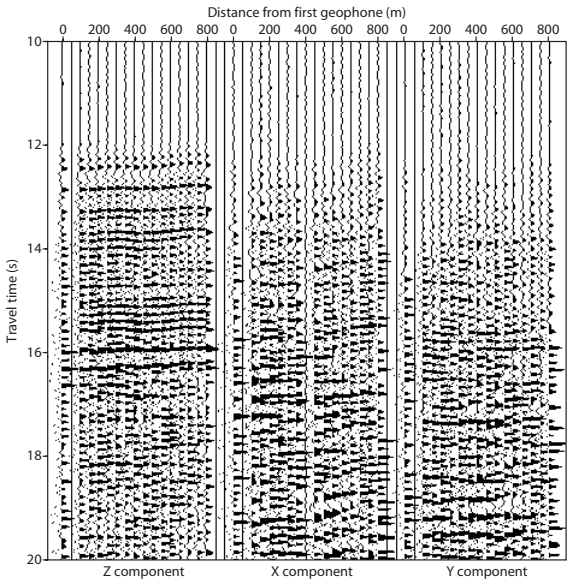

Figure 6: (a) Seismic background-noise panel (number 66) containing nearly horizontal coherent events starting at around 12 s. The left panel shows the vertical component of the particle velocity, the middle panel - the inline component, and the right panel - the crossline component. Note that the arrival at around 12 s appears only in the z-component, ruling out the possibility that this is a surface wave.

Weaver, R. L., and Lobkis, O. I., 2001, Ultrasonics without a source: thermal fluctuation correlations at MHz frequencies, *Physical Review Letters*, **87**, 134301–1–134301–4.